Journal of Molecular Structure: THEOCHEM 862 (2008) 66–73

Contents lists available at ScienceDirect

Journal of Molecular Structure: THEOCHEM

journal homepage: www.elsevier.com/locate/theochem

Environmental effects on molecular conformation: Bicalutamide analogs

Hyun Joo [a], Elfi Kraka [a], Dieter Cremer [b,*]

[a] Department of Chemistry, University of the Pacific, 3601 Pacific Avenue, Stockton, CA 95211, USA
[b] Department of Chemistry and Department of Physics, University of the Pacific, 3601 Pacific Avenue, Stockton, CA 95211, USA

ARTICLE INFO

Article history:
Received 25 March 2008
Received in revised form 22 April 2008
Accepted 23 April 2008
Available online 11 May 2008

Keywords:
Bicalutamide analogs
Prostate cancer
Biostereomer
H-bonding
VCD
Spectra

ABSTRACT

Two bicalutamide analogs (*N*-[4-nitro-3-(trifluoromethyl)phenyl]-3-(4-fluorophenyl)sulfinyl-2-hydroxy-2-methyl-propane-amide **2** and its 4-cyano derivative **3**) with an *R*-configured asymmetric carbon atom and a chiral sulfoxide group are described quantum chemically to determine their properties in dependence of their conformation and their (*R*,*S*)-configuration at the sulfoxide S atom. Compounds **2** and **3** are known to be novel androgen receptor antagonists with biological activities that depend significantly on the configuration of their stereogenic centers. For the purpose of a rapid differentiation between active and less active diastereomers of **2** and **3**, relative energies, conformational preferences in different media, NMR chemical shift values, vibrational spectra, and vibrational circular dichroism (VCD) spectra are calculated for up to 12 different conformers. It is demonstrated that both **2** and **3** prefer strongly different conformations in dependence of the surrounding medium and as a consequence of the change from intra- to intermolecular H-bonding. The different diastereomers can be easily distinguished by specific NMR chemical shifts, infrared bands, or VCD rotational strengths.

© 2008 Elsevier B.V. All rights reserved.

1. Introduction

Prostate cancer is the most common cancer for men in the USA. It is also a major cause of male death in the world [1]. The growth of prostate cancer strongly depends on androgens. Therefore, androgen receptor antagonists are widely used as hormone therapy. Bicalutamide (**1**, Fig. 1), *N*-[4-cyano-3-(trifluoromethyl)phenyl]-3-(4-fluorophenyl)sulfonyl-2-hydroxy-2-methyl-propane-amide, $C_{18}H_{14}F_4N_2O_4S$, marketed as Casodex®, is an androgen receptor antagonist with good efficacy against prostate cancer [2–4]. However, it also has considerable drawbacks in that prostate cancer recurs after a short period of response [5,6]. Under in vitro conditions, bicalutamide has shown partial agonistic activity for androgen receptors at high concentrations. This partial agonistic activity may be one of the factors contributing to the recurrence [5,6]. Therefore, the search for bicalutamide analogs that do not have agonistic activities has been actively pursued and, consequently, many bicalutamide analogs have been reported in the literature [7–11].

Bicalutamide has one chiral center (asymmetric C4 atom with an *R*-configuration) as shown in Fig. 1. The absolute configuration of this chiral center proves to be important because it influences the biological activity of the molecule [7,12–14]. Recently, bicalutamide analogs that contain a sulfoxide group (**2** and **3**, Fig. 1) have been synthesizd [15]. The introduction of the sulfoxide group leads to a second chiral center (starred atoms in Fig. 1) and the formation of two possible diastereomers with *R*- or *S*-configuration at atom S2 abbreviated as C(*R*)S(*R*) (diastereomer **a**) and C(*R*)S(*S*) (diastereomer **b**) in this work. A reliable determination of the absolute configuration of the chiral S=O center is a prerequisite for correctly analyzing the androgen receptor antagonistic activities of these new bicalutamide analogs.

In this work, we investigate with the help of quantum chemical methods how the different diastereomers of bicalutamide derivatives such as **2** or **3** (Fig. 1) can be reliably and rapidly identified with the help of spectroscopic means. This investigation is timely in view of the recent synthesis of **2** and **3** and the need to clarify what diastereomers have been synthesized [15].

In Section 2 we describe the quantum chemical methods we have used for the characterization of the bicalutamide analogs. In Section 3, the most stable conformations in the gas phase and in a polar solvent are determined and their dependence on the environment is discussed. Although we have used water as a solvent in the second case, we note that **1** and its analogs are practically insoluble in water [7–11,15]. Therefore the situation of a solvent with high dielectric constant is chosen in this work only for the purpose of assessing the whole range of conformational changes in dependence of the medium. Focusing on the most stable conformations in a medium with low dielectric constant, NMR chemical shifts, vibrational spectra, and vibrational circular dichroism (VCD) spectra are calculated and analyzed to determine if they provide tools for rapidly distinguishing between the diastereomers of bicalutamide analogs.

* Corresponding author. Tel.: +1 2099462601.
E-mail address: dcremer@pacfic.edu (D. Cremer).

0166-1280/$ - see front matter © 2008 Elsevier B.V. All rights reserved.
doi:10.1016/j.theochem.2008.04.037

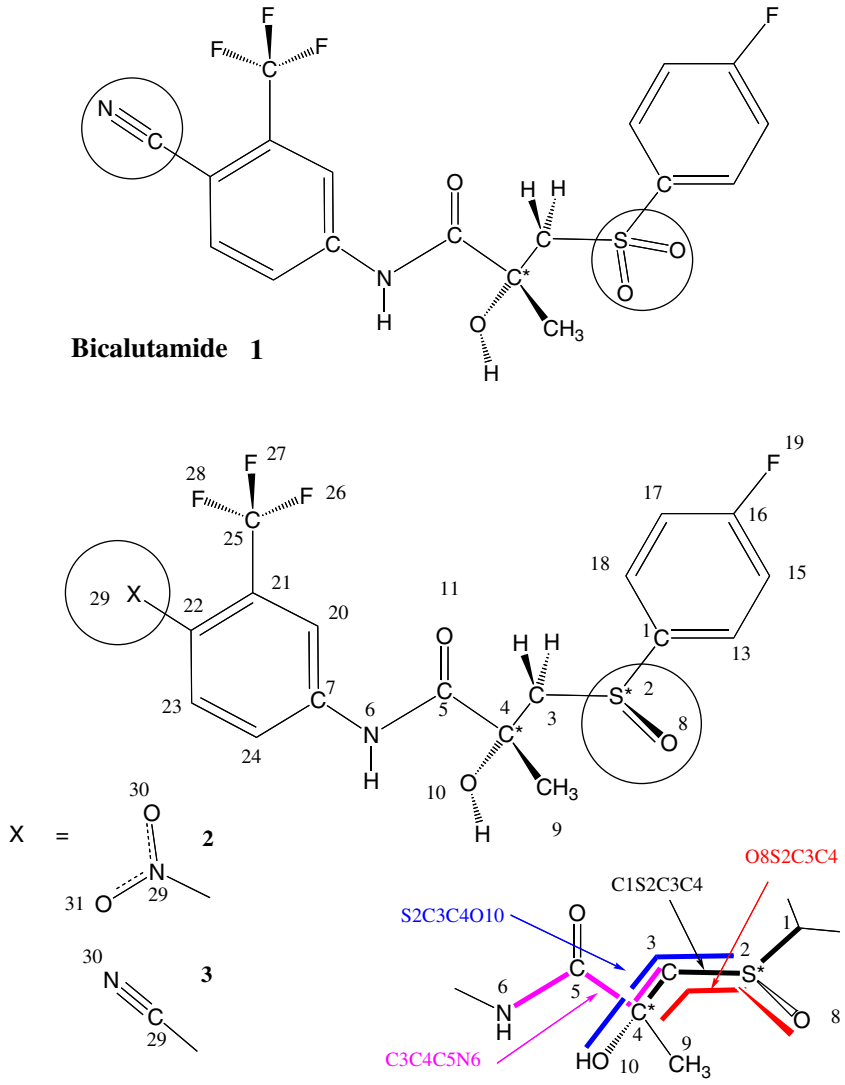

Fig. 1. Bicalutamide, **1**, and its sulfoxide analogs **2** and **3**. Numbering of atoms and dihedral angles used to describe the conformation of the link between the phenyl rings.

2. Computational methods

Since compounds **2** and **3** possess a flexible link between the *p*-fluoro-phenyl and the *m*-trifluoromethyl-phenyl group, it is difficult to predict the most stable conformations of the two diastereomers without extensive scanning of their conformational energy surface: For the purpose of facilitating this task semiempirical calculations were combined with density functional theory (DFT) calculations following a five-step procedure. (a) A conformational model was chosen for bicalutamide analogs **2** and **3**, in which both phenyl groups and the peptide unit were kept planar. (b) The AM1 method [16] was used to scan the conformational energy surface in the directions of the dihedral angles driving rotations at bond C1S2, S2C3, and C3C4 (see Fig. 1). (c) Two positions of the 4-nitro- or cyano-substituted 3-(trifluoromethyl)phenyl ring with the CF_3 group being syn or anti to the C=O group (phenyl flip) were investigated. (d) The rotor groups CH_3, CF_3, NO_2, and OH were adjusted for each conformation considered by appropriate AM1 geometry optimizations. The procedure (a–d) led to global and local conformational minima of the diastereomers of **2** and **3** on a 10-dimensional conformational energy surface at the AM1 level of theory. (e) The most stable AM1 conformers of each diastereomer were completely reoptimized using DFT with the B3LYP hybrid functional [17–19] and Pople's 6-31G(d,p) basis set (involving up to 495 basis functions) [20]. In this way, for each diastereomer four stable conformers were identified, of which those just differing by a phenyl flip (the **a**′ or **b**′ conformers) were not further investigated for compound **3** thus limiting the total number of investigated conformers to **12**.

The conformers calculated in this way are characterized by four dihedral angles: C1S2C3C4, O10C4C3S2, C4C3S2O8, and C3C4C5N6 (for numbering of atoms, see Fig. 1), which can be either syn-periplanar (sp, dihedral angle values of 0 ± 30°), syn-clinal (sc, ±60 ± 30°), anti-clinal (ac, ±120 ± 30°), or anti-periplanar (ap, 180 ± 30°). The angle O10C4C3S2 was chosen rather than angle C5C4C3S2 (the latter is related to the former) because the position of O10 (in connection with that of O8 given by dihedral angle C4C3S2O8) determines the possibility of O10H...O8S2 H-bonding. For rapid identification of the different conformers, we will classify the calculated dihedral angles by the stereochemical acronyms sc, sp, ac, and ap.

For the conformational forms investigated, harmonic vibrational frequencies were calculated at B3LYP/6-31G(d,p) to verify the nature of all stationary points and to determine vibrational and temperature corrections for the energy differences. Vibrational frequencies were scaled with the factor 0.96. In all cases, energy differences ΔE at 0 K, enthalpy differences $\Delta H(298)$, entropies $S(298)$, and free energy differences $\Delta G(298)$ at 298 K were determined relative to the most stable conformer.

The quantum chemical description of **2** and **3** obtained in this way refers to the gas phase situation and identifies the electronic effects determining their geometry and stability. Experiments for bicalutamide and its analogs are carried out in various solvents including pentane and $CHCl_3$. In view of the low dielectric constants of these solvents ($\varepsilon = 1.84$; 4.81 [21]), the gas phase ($\varepsilon = 1$) results are also relevant for the experimental studies. However, we wanted to determine the full range of conformational changes possible by using solvents of high dielectric constants and therefore we have also considered the situation in aqueous solution (water: $\varepsilon = 78.39$ [21]) despite the fact that bicalutamide and its analogs are hardly soluble in this solvent. We calculated solvation free energies for the diastereomers of **2** and **3** employing the conductor-like polarizable continuum model (CPCM) of Cossi and coworkers [22]. In view of the limited role of water as a solvent for **2** and **3**, no attempt was made to reoptimize the investigated forms in this medium.

For NMR chemical shift calculations the DFT-IGLO method of Cremer and Olsson [23] was used that employs orbital corrections similar but not identical to those suggested by Malkin and co-workers [24]. For the purpose of calculating ^{1}H and ^{13}C NMR chemical shifts, the magnetic shielding values of TMS were used as reference. For the hetero nuclei ^{15}N, ^{17}O, ^{19}F, and ^{33}S, calculated magnetic shielding of NH_3, H_2O, HF, and CS_2 were determined and the following equations were applied

$$\delta(^{17}O) = \sigma(H_2O) - \sigma - 36.1 \quad (1)$$

$$\delta(^{19}F) = \sigma(HF) - \sigma - 221.4 \quad (2)$$

$$\delta(^{33}S) = \sigma(CS_2) - \sigma - 334.2 \quad (3)$$

to comply with experimental standards [25–27]. In addition to the NMR chemical shifts, infrared and VCD spectra [28,29] were calculated for all diastereomers investigated using the B3LYP/6-31G(d,p) methodology. For the identification of a given diastereomer, the infrared and VCD spectra of the most stable conformers were combined using weight factors derived from their free energy differences at 298 K. All calculations were carried out with the program packages COLOGNE08 [30] and Gaussian 03 [31].

3. Results and discussion

The low energy conformers obtained for the diastereomers of **2** and **3** are shown in Figs. 2 and 3. Relative energies (enthalpies, free energies) in the gas phase and in aqueous solution and dipole moments are listed in Table 1. The most stable conformer for diastereomer **2b** is **2b-1'** that has almost the same energy as **2b-1**, the form with the 180-rotated 4-nitro-3-(trifluoromethyl)phenyl group at the peptide unit ($\Delta E = 0.2$ kcal/mol, $\Delta H = \Delta G = 0$ kcal/mol, Table 1). The stability of the C(*R*)S(*S*) configuration is a result of a relatively strong OH···OS H-bond (H,O distance: 1.790 Å; Fig. 2) supported by attractive NH···O and CH···O═C interactions as shown in Fig. 2. The C1S2C3C4 dihedral angle is close to 180° (ap-conformation), which leads to a stretched overall-shape of the molecule. The calculated dipole moments for **2b-1** and **2b-1′** are relatively large (8.7 and 9.1 D, Table 1) which indicates that solvation of these diastereomers with a polar solvent such as water leads to some extra stability. This is confirmed by the fact that **2b-1** and **2b-1′** represent also the most stable conformers in aqueous solutions (Table 1).

As soon as the dihedral angle C1S2C3C4 is reduced, the SO group is rotated away from the hydroxyl group and the OH···OS H-bond is broken thus leading to the conformer **2b-2** with dihedral angle C1S2C3C4 close to 54° and a U-shaped form, which has a significantly higher energy ($\Delta G(298) = 10.4$ and $\Delta G(\text{water}) = 6.7$ kcal/mol) in the gas phase and aqueous solution.

For the C(*R*)S(*R*) configuration **2a**, OH···OS H-bonding is not possible in any of the stretched forms that occupy local minima on the conformational energy surface of the molecule (**2a-1**, **2a-2**, Fig. 2). The molecule has to rotate from the ap-C1S2C3C4 to the sc-C1S2C3C4 conformation with a dihedral angle close to 70° to reestablish OH···OS H-bonding (**2a-3** and **2a-3′**, H,O distance: 1.725 Å, Fig. 1). This leads to two U-shaped forms and a decrease in energy from 6.7 to 1.9 and 5.6 to 2.2 kcal/mol relative to the free energy of **2b-1** (**2b-1′**, Table 1) as calculated for the gas phase. The dipole moments decrease in this way from 11 to 11.8 D to 6.9 to 7.6 D indicating that solvation in a polar solvent may change relative stabilities. Indeed, the curled U-forms **2a-3** and **2a-3′** turn out to be less stable in aqueous solution (4.1 and 4.9 kcal/mol) than the stretched forms **2a-1** and **2a-2** (1.3 and 2.1 kcal/mol, Table 1). This is reasonable because intramolecular H-bonding can be replaced in water by intermolecular H-bonding and the molecular form with the larger dipole moments will benefit more strongly from solvent stabilization as verified in this work by CPCM calculations.

By replacing the NO_2 group by a CN group thus leading to diastereomers **3a** and **3b** (Fig. 1), similar geometries and relative energies are obtained (Table 1, Fig. 3). The investigation of **3** was desirable in view of the fact that bicalutamide carries a cyano rather than a nitro group in position 4 of the 3-(trifluoromethyl)phenyl ring. Hence, molecule **3** is the actual link to bicalutamide and helps to compare biological activity in dependence of an exchange of SO_2 against SO (Fig. 1).

We conclude that for the C(*R*)S(*R*) diastereomer **2a** (**3a**) different conformations dominate in different media. In the gas phase as well as nonpolar solvents with low dielectric constant, the U-forms **2a-3** and **2a-3′** will be in a conformational equilibrium with other low energy forms (**2a-1**, **2a-2**; calculated barriers are below 3 kcal/mol), however the former conformations will be preferentially populated according to the calculated $\Delta G(298)$ values (Table 1). In polar solvents such as water, this role is taken over by the stretched forms **2a-1** and **2a-2** in a distribution 80:20. Independent of the medium, for the C(*R*)S(*S*) configuration, there will be always a dominance of the stretched forms **2b-1** and **2b-1′**. This has to be considered when searching for suitable properties by which diastereomers of **2** (or **3**) can be distinguished.

4. NMR spectroscopy: chemical shifts

The NMR chemical shifts of all conformers were calculated in this work (see Supporting Information). However, we will discuss only the chemical shifts of the most stable conformers in the gas phase. This has to do with the fact that the target compounds **2** and **3** possess little solubility in water and therefore have to be investigated in nonpolar solvents such as pentane or chloroform. Because of the low dielectric constants of these solvents, chemical shifts measured in chloroform or pentane do not differ significantly from gas phase values.

In Table 2, those chemical shifts, that make it possible to identify individual diastereomers of **2** (or **3**) in a mixture of reaction products, are listed. All calculated NMR chemical shifts including those of the heteroatoms are given in Figures A1 to A4 of the Supporting Information. There are just small chemical shift differences between those conformers that are related by a phenyl flip (180° rotation of the 4-nitro-3-(trifluoromethyl)phenyl group) so that a distinction of conformers **2b-1** and **2b-1′** or **2a-3** and **2a-3′** in a mixture is difficult. However apart from the phenyl flip, the most stable forms of the diastereomers of **2** and **3** can clearly be distinguished with the help of their NMR chemical shifts.

In the ^{13}C NMR spectra, the chemical shift of C3, the atom between the two chiral centers, is at 47 ppm for **2a-3**, however at 56 ppm for **2b-1**. The attached H atoms at C3 possess NMR chem-

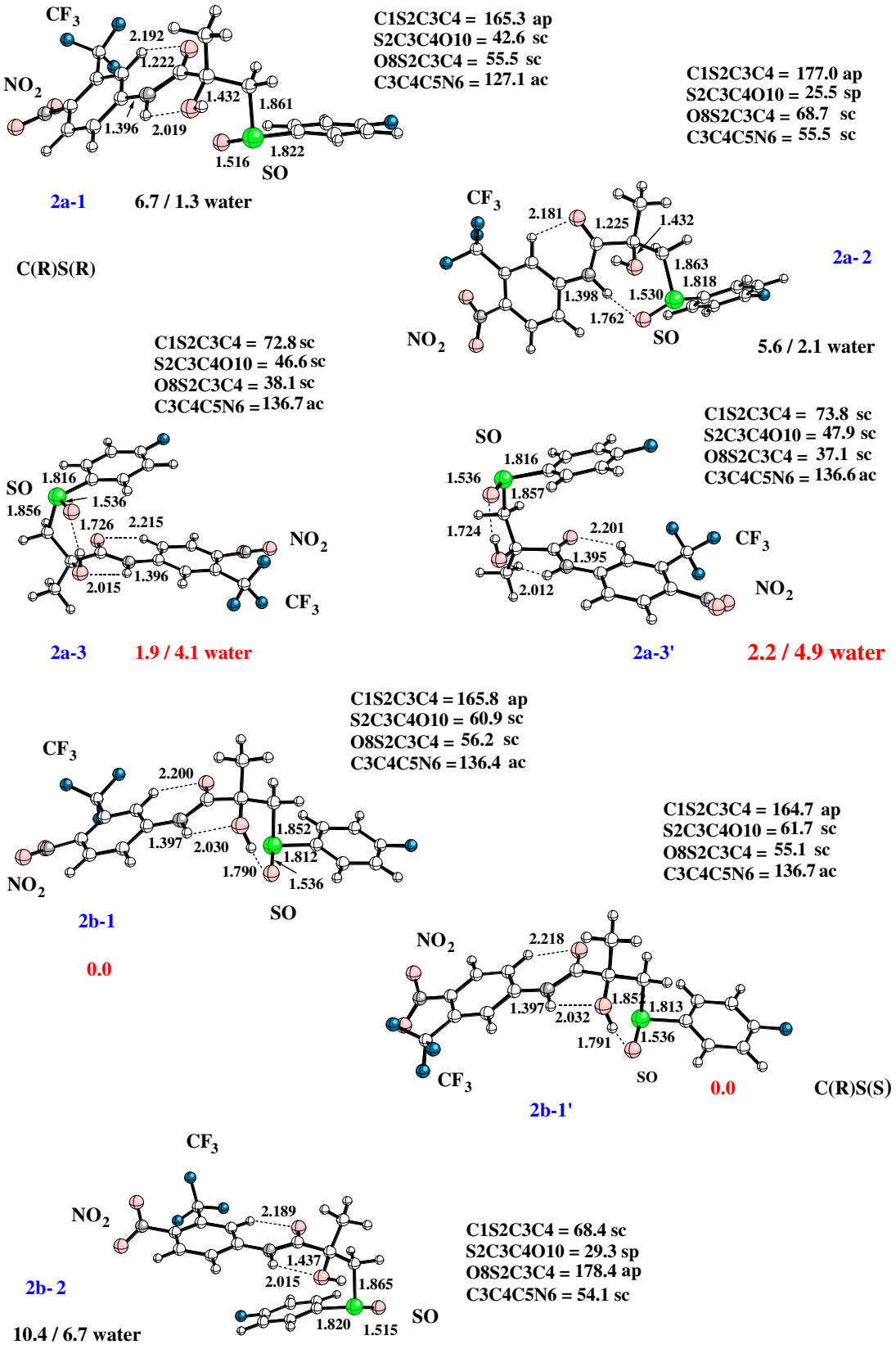

Fig. 2. B3LYP/6-31G(d,p) geometries of conformers **2a-1, 2a-2, 2a-3, 2a-3′**, **2b-1**, **2b-1′**, and **2b-2**. Bond lengths in Å, bond angles in deg. C and H atoms are given as white balls, N atom in black, O atoms in red, F atoms in blue, S atom in green. The relative free energies in the gas phase and in aqueous solution are also given (most stable conformers in the gas phase: red values). For the notation of the dihedral angles, see Fig. 1. (For interpretation of the references to color in this figure legend, the reader is referred to the web version of this paper.)

ical shifts of 3.1 and 3.1 ppm in the first case and 2.1 and 3.2 ppm in the second case, i.e., that the shift difference increases to 1 ppm when the molecule adopts a stretched conformation (compare also the corresponding shift values for **3a-3** and **3b-2**, Table 2).

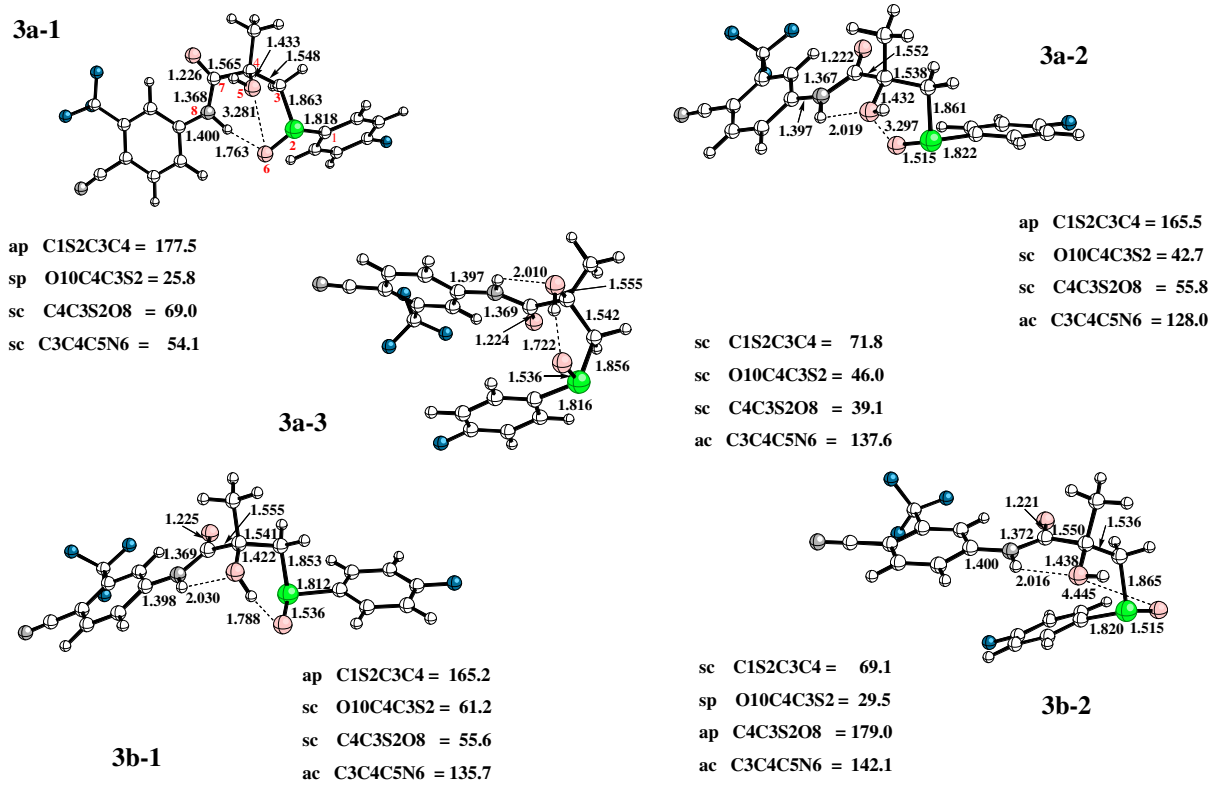

Fig. 3. B3LYP/6-31G(d,p) geometries of conformers **3a-1, 3a-2, 3a-3, 3b-1**, and **3b-2**. Bond lengths in Å, bond angles in deg. C and H atoms are given as white balls, N atom in black, O atoms in red, F atoms in blue, S atom in green. For the notation of the dihedral angles, see Fig. 1. (For interpretation of the references to color in this figure legend, the reader is referred to the web version of this paper.)

Table 1
Zero point energies (ZPE), entropies *S*, dipole moments μ, relative energies ΔE, relative enthalpies $\Delta H(298)$, relative free energies $\Delta G(298)$, and relative free energies in aqueous solution $\Delta G(sol)$ for the most stable conformations of diastereomers **2a**, **2b**, and **3a**, **3b**[a]

X	Molecule	Configuration	Overall-shape	Conformation	ZPE	*S*	μ	ΔE	$\Delta H(298)$	$\Delta G(298)$	$\Delta G(sol)$
NO_2	**2a-1**	C(R)S(R)	stretched	ap-sc-sc-ac	189.0	187.0	11.79	7.8	7.5	6.7	1.3
	2a-2		stretched	ap-sp-sc-sc	189.2	184.7	10.97	6.0	5.7	5.6	2.1
	2a-3		U-form	sc-sc-sc-ac	189.8	181.8	7.61	1.2	1.2	1.9	4.1
	2a-3′		U-form	sc-sc-sc-ac	189.8	181.4	6.94	1.5	1.4	2.2	4.9
	2b-1	C(R)S(S)	stretched	ap-sc-sc-ac	189.7	184.8	8.67	0.2	0.2	0.0	0.0
	2b-1′		stretched	ap-sc-sc-ac	189.8	184.3	9.15	0.0	0.0	0.0	0.0
	2b-2		U-form	sc-sc-ap-sc	189.2	184.8	8.22	10.9	10.6	10.4	6.7
CN	**3a-1**	C(R)S(R)	stretched	ap-sc-sc-ac	186.5	183.8	11.88	7.7	7.4	6.9	1.5
	3a-2		stretched	ap-sp-sc-sc	186.7	182.0	11.05	5.9	5.6	5.7	2.3
	3a-3		U-form	sc-sc-sc-ac	187.3	177.8	6.97	1.3	1.3	2.6	5.2
	3b-1	C(R)S(S)	stretched	ap-sc-sc-ac	187.1	182.1	8.78	0.0	0.0	0.0	0.0
	3b-2		U-form	sc-sp-ap-ac	186.6	182.9	8.32	10.6	10.4	10.2	6.4

[a] Relative energies (enthalpies, free energies) and zero-point energy (ZPE) values in kcal/mol, entropy *S* in entropy units, dipole moments μ in Debye. ΔE, $\Delta H(298)$, $\Delta G(298)$, and $\Delta G(sol)$ give the energy difference at 0 K without ZPE correction, the enthalpy difference at 298 K, the free energy difference at 298, and the difference in the solvation free energies with regard to the most stable form, **2b-1′**. For the overall-shape, see text. Conformations are given in terms of dihedral angle (see Fig. 1) using standard conformational abbreviations: syn-periplanar (sp, 0 ± 30°), syn-clinal (sc, ±60 ± 30°), anti-clinal (ac, ±120 ± 30°), or anti-periplanar (ap, 180 ± 30°).

The comparison of calculated to measured proton shifts is difficult because the influence of solvent effects changes the proton spectrum considerably. However in a nonpolar solvent with low dielectric constant, the trends calculated in this work should be also observed experimentally. Furthermore, it should be possible to identify the U-form of **2a-3** via the chemical shifts of its aromatic protons. In the stretched conformation (**2a-1, 2a-2, 2b-1**), the signals of these protons appear between 7.3 and 9.4 ppm. However, in the U-forms (**2a-3, 2b-2**), there is some stacking between the phenyl rings so that some of the aromatic protons are positioned exactly above the second phenyl ring in the molecule. These protons are shielded and resonate at lower δ values. In total the aromatic protons are upfield shifted to 6.6–8.6 ppm, which should be clearly seen in the proton NMR.

If one includes also ^{17}O and ^{33}S NMR chemical shifts (Table 2), all conformations become distinguishable. There are shift differences of 20, 10, and 30 ppm with regard to the δ values of O8 when comparing **2a-3** with (**2a-2, 2a-1**), **2b-1** and **2b-2**. This does not make it possible to distinguish between **2a-1** and **2a-2**, however inclusion of the NMR chemical shifts of O10 and S2 (^{17}O values: 2.4 and −14.1 ppm; ^{33}S: −181.4 and −190.4 ppm, Table 2) solves the problem.

Similar trends in the calculated NMR chemical shift values are observed for molecule **3**. Hence it is possible to distinguish

Table 2
Calculated NMR chemical shifts of selected nuclei of **2** and **3**[a]

Molecule	(C3)H1	(C3)H2	Aromatic protons	C3	O8	O10(H)	S2
2a-1	2.2	3.2	7.0–9.3	61.9	−24.8	−14.1	−190.4
2a-2	2.5	2.6	7.4–9.2	61.6	−23.9	2.4	−181.4
2a-3	3.1	3.1	6.7–8.4	47.1	−43.5	−41.8	−165.6
2a-3′	3.2	3.2	6.6–8.6	47.4	−44.3	−40.3	−164.7
2b-1	2.1	3.2	7.1–9.7	55.9	−33.2	−34.4	−178.8
2b-1′	2.2	3.2	7.4–9.4	55.7	−33.6	−33.8	−180.2
2b-2	2.6	3.3	6.6–8.9	61.7	−11.4	−10.7	−181.1
3a-1	2.2	3.3	7.0–9.4	61.9	−24.9	−13.9	−189.7
3a-2	2.5	2.7	7.4–9.3	61.6	−24.0	2.3	−181.4
3a-3	3.1	3.2	6.9–8.4	47.0	−43.1	−42.5	−165.5
3b-1	2.1	3.3	7.1–9.6	55.9	−33.6	−34.2	−180.1
3b-2	2.6	3.3	6.5–8.7	61.8	−11.8	−10.6	−180.1

[a] All NMR chemical shifts in ppm. Values in red belong to the conformers most stable in the gas phase and in non-polar solvents. References are TMS for ^{13}C and ^{1}H, H_2O for ^{17}O, and CS_2 for ^{33}S chemical shifts. See Eqs. (1) and (3). B3LYP/6-31G(d,p) calculations. Values of the most stable conformers in red. (For interpretation of the references to color in this table, the reader is referred to the web version of this paper.)

between the diastereomers of **2** (**3**) in their most stable conformations utilizing NMR spectroscopy. With the help of the NMR chemical shift values determined in this work, it should be possible to determine which of the diastereomers possess a C(*R*)S(*R*) (the **a**-forms) and which a C(*R*)S(*S*) configuration (the **b**-forms). Because the exchange of the nitro against a cyano group does not lead to any major charges in the properties of the bicalutamide analog, we will discuss in the following only the results obtained for **2**.

5. Vibrational spectroscopy: infrared and VCD spectra

The calculated infrared spectra reveal some significant differences between the diastereomers **2a** and **2b**. The O-H stretching frequencies for **2a-3 and 2a-3'** are calculated to be 3238 and 3241 cm^{-1} (scaled values), respectively, whereas **2b-1** and **2b-1′** are characterized by values of 3309 and 3306 cm^{-1}. This significant red shift in the O-H stretching frequency of the C(*R*)S(*R*) configuration **2a** is due to the stronger hydrogen bonding between OH and O═S group.

Fig. 4 gives a superposition of the infrared spectra of the most stable conformers of **2a** (i.e. adding the two spectra with 60% of the infrared intensity of **2a-3** and 40% of that of **2a-3′**) and **2b** (50% of the infrared intensity of **2b-1** and 50% of that of **2b-1′**) in the range from 800 to 1800 cm^{-1}. There are three areas where the two spectra differ in a distinctive way (Fig. 4): (a) 1120 to 1130 cm^{-1} (**2a-3** + **2a-3**: 1 small band with shoulder; **2b-1** + **2b-1′**: 1 somewhat more intense band); (b) 1200 to 1240 cm^{-1} (**2a-3** + **2a-3'**: 2 small bands; **2b-1** + **2b-1'**: 1 somewhat more intense band); (c) 1380 to 1480 cm^{-1} (**2a-3** + **2a-3′**: 5 small bands; **2b-1** + **2b-1′**: 3 somewhat more intense bands). These differences should be sufficient to distinguish between diastereomers **2a** and **2b** in nonpolar solvents with low dielectric constant.

The VCD spectra of diastereomers **2a** and **2b** depend on their conformation and on the absolute configuration at the two chiral centers. Therefore, knowledge of the VCD spectra guarantees an identification of the diastereomers. As in the case of the vibrational spectra, first the VCD spectrum of each stable conformer was calculated (see Supporting Information) and then the spectra of the two

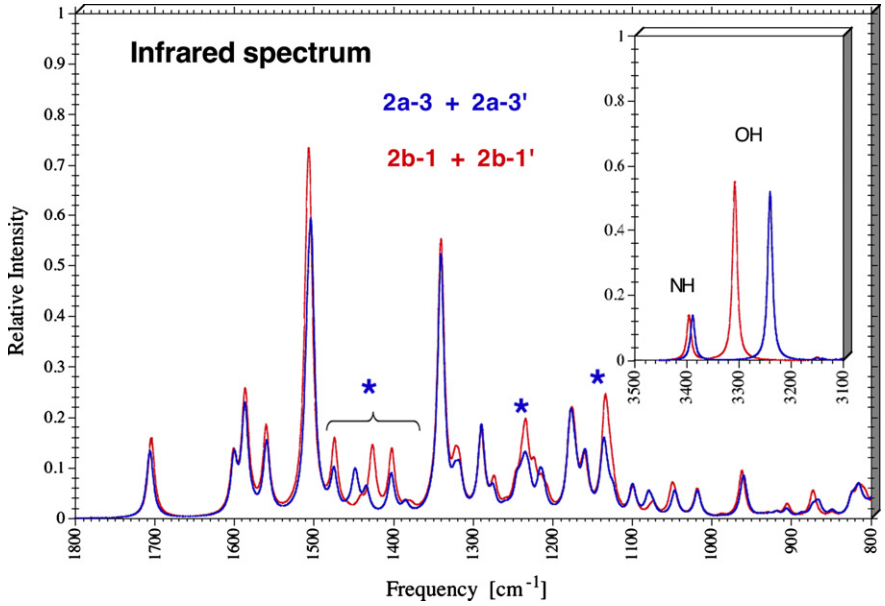

Fig. 4. Superimposed infrared spectra of diastereomers **2a** (blue) and **2b** (red). For **2a**, an equilibrium of conformers **2a-3** and **2a-3'** is calculated with a 40% to 60% population of the two conformers, whereas for **2b** a 50:50 equilibrium between **2b-1** and **2b-1′** was used according to the calculated $\Delta G(298)$ values of Table 1. The range between 800 and 1800 cm^{-1} is given. The insert gives the range of the NH and OH stretching frequencies. For the individual infrared spectra of **2a-3**, **2a-3′**, **2b-1,** and **2b-1′**, see the Supporting information. Stars indicate frequency ranges that differ for the two diastereomers. The relative intensity of 1.0 was determined for the conformer with the strongest intensity and used as a reference for all other spectra. (For interpretation of the references to color in this figure legend, the reader is referred to the web version of this paper.)

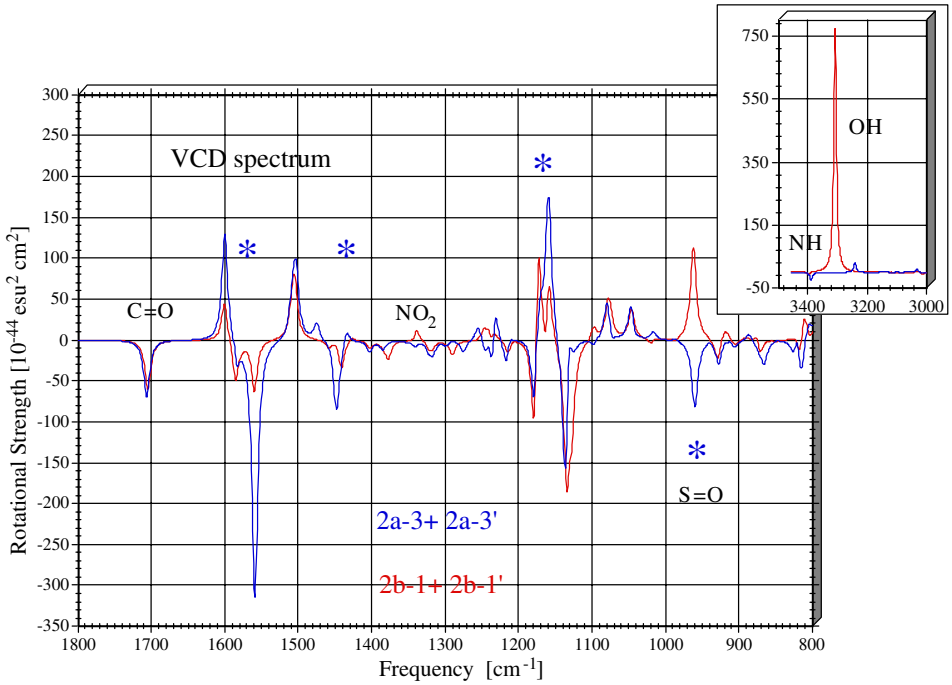

Fig. 5. Superimposed vibrational circular dichroism (VCD) spectra of diastereomers **2a** (blue) and **2b** (red). For **2a**, an equilibrium of conformers **2a-3** and **2a-3′** is calculated with a 40% to 60% population of the two conformers, whereas for **2b** a 50:50 equilibrium between **2b-1** and **2b-1′** was used according to the calculated $\Delta G(298)$ values of Table 1. The range between 800 and 1800 cm^{-1} is given. The insert gives the range of the NH and OH stretching frequencies. For the individual VCD spectra of **2a-3**, **2a-3′**, **2b-1,** and **2b-1′**, see the Supporting information. Stars indicate frequency ranges that differ for the two diastereomers. (For interpretation of the references to color in this figure legend, the reader is referred to the web version of this paper.)

Table 3
Important harmonic vibrational frequencies (scaled by 0.96, cm^{-1}), infrared intensities (in parentheses, km/mol), and optical rotational strengths (italic values, $\times 10^{-44}$ esu^2 cm^2) for the most stable conformers of diastereomers **2a** and **2b**

Vibrational Stretching mode	**2a-3** C(R)S(R)	**2a-3'** C(R)S(R)	**2b-1** C(R)S(S)	**2b-1'** C(R)S(S)
C=O	1706	1708	1704	1706
	(129.4)	(124.2)	(154.1)	(146.6)
	−75.5	*−66.9*	*−64.6*	*−59.7*
NO_2	1341	1340	1341	1339
	(441.4)	(530.5)	(465.4)	(573.6)
	−10.6	*−1.3*	*−26.5*	*48.1*
S=O	961	959	962	962
	(74.3)	(86.7)	(81.3)	(89.4)
	−76.0	*−87.5*	*126.3*	*104.6*
O−H	3241	3238	3309	3306
	(522.0)	(510.0)	(538.7)	(551.0)
	45.9	*7.9*	*835.5*	*807.2*
N−H	3388	3390	3396	3396
	(128.3)	(135.3)	(126.4)	(132.0)
	−25.0	*−25.9*	*−10.1*	*−6.1*

most stable conformers combined using weight factors that are directly calculated from the free energy difference of the conformers in question. The spectra thus obtained are shown in Fig. 5.

There are characteristic differences between diastereomers **2a** and **2b** with regard to the optical rotational strength of the S=O and O—H stretching modes (Table 3). For **2a-3** and **2a-3′** with their C(*R*)S(*R*) configuration**,** the S=O stretching mode possesses optical rotational strengths of −76.0 and −87.5 $\times 10^{-44}$ esu^2 cm^2, however the C(*R*)S(*S*) forms **2b-1** and **2b-1′** have rotational strengths of 126.3 and 104.6 $\times 10^{-44}$ esu^2 cm^2. The change in sign is caused by the absolute configuration at sulfur. Also, the O—H stretching mode reveals a dramatic difference in the rotational strength (from 8 to 46, 807, and 835 $\times 10^{-44}$ esu^2 cm^2 in the sequence **2a-3′**, **2a-3**, **2b-1′**, **2b-1**, Table 3 and Fig. 5), which provides a simple indicator for the absolute configuration at chiral center S2. The rotational strength associated with the C=O stretching motion, however, does differ less on the absolute configuration and conformation of **2** and therefore is not a suitable indicator (Fig. 5 and Table 3). The differences in the rotational strengths of the NO stretching mode (Table 3) are larger where it helps again that **2b-1′** has a positive value of 48 $\times 10^{-44}$ esu^2 cm^2 so that this conformation can be easily distinguished from the three others (see also Fig. 5).

Strong differences between the diastereomers **2a** and the **2b** are found in the ranges 1120–1170 cm^{-1}, 1380–1480 cm^{-1}, and 1560–1600 cm^{-1}, which are associated with CH_2 bending, phenyl ring stretching, CH_3 wagging, and other framework motions. Based on the VCD spectra (see Fig. 5) diastereomers **2a** and **2b** should be easily identified.

6. Conclusions

We have shown that the diastereomers **2a** and **2b** prefer different conformations in the gas phase (corresponding to the situation in nonpolar solvents with low dielectric constant) and in strongly polar solvents. Intramolecular H-bonding between the OH and SO groups leads in the case of **2a** to a U-form (**2a-3** and **2a-3′**), which in a polar medium stretches out replacing intramolecular by intermolecular H-bonding (**2a-1** and **2a-2**). The *S*-configuration at the chiral S(=O) center makes OH···SO H-bonding possible in the stretched (**2b-1** and **2b-1′**) rather than the U-form **2b-2** possible, which explains the change in the conformational behavior in the case of diastereomer **2b**. This holds for both gas phase, nonpolar and polar solvents. Similar trends are observed for bicalutamide **3**. Rapid identification of the different diastereomers of **2** or **3** can be best accomplished with the help of VCD rotational strengths, infrared spectra or NMR chemical shifts, which reflect the fact that U- and stretched forms possess different spectroscopic properties.

We note that the formation of H-bonding determines the relative stabilities of the C(*R*)S(*R*) and C(*R*)S(*S*) diastereomers and will also play a role as for the relative stabilities of the transition states leading to the formation of **2a** and **2b** (**3a** and **3b**). Hence, the experimentally observed preference of the formation of the C(*R*)S(*S*) diastereomer **b** [15] and its larger stability can be connected to the impact of strong OH···SO interactions. The larger biological activity of **2a** (**3a**) [15] as compared to **2b** (**3b**) can be connected to its more spherical shape. These results are relevant for the synthesis, identification, and application of bicalutamide analogs **2** and **3**.

Acknowledgements

Useful discussions with Dr. Wei Li, University of Tennessee, are acknowledged. E.K. and D.C. thank the National Science foundation and the University of the Pacific for support.

Appendix A. Supplementary data

Supplementary data associated with this article can be found, in the online version, at doi:10.1016/j.theochem.2008.04.037.

References

[1] D.M. Parkin, F. Bray, J. Ferlay, P. Pisani, Cancer J. Clin. 55 (2005) 74.
[2] P.F. Schellhammer, J.W. Davis, Clin. Prostate Cancer 2 (2004) 213.
[3] G.J. Kolvenbag, G.R. Blackledge, Urology 47 (1996) 70 (1A Suppl., 80).
[4] J.T. Dalton, A. Mukherjee, Z. Zhu, L. Kirkovsky, D.D. Miller, Biochem. Biophys. Res. Commun. 244 (1998) 1.
[5] Recent Advances in Prostrate Cancer and BPH, F.H. Schröder, Ed., Parthenon, New York, 1997.
[6] C.W. Gregory, B. He, R.T. Johnson, O.H. Ford, J.L. Mohler, F.S. French, E.M. Wilson, Cancer Res. 61 (2001) 4315.
[7] K.D. James, N.N. Ekwuribe, Synthesis 7 (2002) 850.
[8] V.A. Nair, S.M. Mustafa, M.L. Mohler, J.T. Dalton, D.D. Miller, Tetrahedron Lett. 47 (2006) 3953.
[9] V.A. Nair, S.M. Mustafa, M.L. Mohler, J. Yang, L.I. Kirkovsky, J.T. Dalton, D.D. Miller, Tetrahedron Lett. 46 (2005) 4821.
[10] V.A. Nair, S.M. Mustafa, M.L. Mohler, S.J. Fisher, J.T. Dalton, D.D. Miller, Tetrahedron Lett. 51 (2004) 9475.
[11] R. Patil, W. Li, C.R. Ross, E. Kraka, D. Cremer, M.L. Mohler, J.T. Dalton JT, D.D. Miller, Tetrahedron Lett. 47 (2006) 3941.
[12] C.A. Marhefka, W. Gao, K. Chung, J. Kim, Y. He, D. Yin, C. Bohl, J.T. Dalton, D.D. Miller, J. Med. Chem. 47 (2004) 993.
[13] L. Kirkovsky, A. Mukherjee, D. Yin, J.T. Dalton, D.D. Miller, J. Med. Chem. 43 (2000) 581.
[14] D.J. Hwang, J. Yang, H. Xu, I.M. Rakov, M.L. Mohler, J.T. Dalton, D.D. Miller, Bioorg. Med. Chem. 14 (2006) 6525.
[15] W. Li, private communication.
[16] M.J.S. Dewar, C.H. Reynolds, J. Comp. Chem. 7 (1986) 140.
[17] A.D. Becke, J. Chem. Phys. 98 (1993) 5648.
[18] A.D. Becke, Phys. Rev. A 38 (1988).
[19] C. Lee, W. Yang, R.G. Parr, Phys. Rev. B 37 (1988) 785.
[20] [a] P.C. Hariharan, J.A. Pople, Theo. Chim. Acta 28 (1973) 213;
[b] M.M. Francl, W.J. Pietro, W.J. Hehre, J.S. Binkley, M.S. Gordon, D.J. DeFrees, J.A. Pople, J. Chem. Phys. 77 (1982) 3654.
[21] Handbook of Chemistry and Physics, 72nd ed., D.R. Lide, Ed., CRC Press, Boca Raton, 1992.
[22] M. Cossi, N. Rega, G. Scalmani, V. Barone, J. Comp. Chem. 24 (2003) 669.
[23] [a] L. Olsson, D. Cremer, J. Phys. Chem. 100 (1996) 16881;
[b] L. Olsson, D. Cremer, J. Chem. Phys. 105 (1996) 8995.
[24] V.G. Malkin, O.L. Malkina, M.E. Casida, D.R. Salahub, J. Am. Chem. Soc. 116 (1994) 5898.
[25] S. Berger, S. Braun, H.-O. Kalinowski, NMR spectroscopy of nonmetals, Thieme, vol. 2, ^{15}N-NMR Spectroscopy, New York, 1992.
[26] S. Berger, S. Braun, H.-O. Kalinowski, NMR spectroscopy of nonmetals, Thieme, vol. 1, ^{17}O-, ^{33}S-, ^{129}Xe-NMR Spectroscopy, New York, 1992.
[27] S. Berger, S. Braun, H.-O. Kalinowski, NMR spectroscopy of nonmetals, Thieme, vol. 4, ^{19}F-NMR Spectroscopy, New York, 1994.
[28] J.R. Cheeseman, M.J. Frisch, F.J. Devlin, P.J. Stephens, Chem. Phys. Lett. 252 (1996) 211.
[29] P.J. Stephens, F.J. Devlin, Chirality 12 (2000) 172.
[30] E. Kraka, J. Gräfenstein, M. Filatov, H. Joo, D. Izotov, J. Gauss, Y. He, A. Wu, V. Polo, L. Olsson, Z. Konkoli, Z. He, D. Cremer, COLOGNE08, University of Pacific, Stockton, CA, 2008.
[31] M.J. Frisch, G.W. Trucks, H.B. Schlegel, G.E. Scuseria, M.A. Robb, J.R. Cheeseman, J.A. Montgomery, Jr., T. Vreven, K.N. Kudin, J.C. Burant, J.M. Millam, S.S. Iyengar, J. Tomasi, V. Barone, B. Mennucci, M. Cossi, G. Scalmani, N. Rega, G.A. Petersson, H. Nakatsuji, M. Hada, M. Ehara, K. Toyota, R. Fukuda, J. Hasegawa, M. Ishida, T. Nakajima, Y. Honda, O. Kitao, H. Nakai, M. Klene, X. Li, J.E. Knox, H.P. Hratchian, J.B. Cross, V. Bakken, C. Adamo, J. Jaramillo, R. Gomperts, R.E. Stratmann, O. Yazyev, A.J. Austin, R. Cammi, C. Pomelli, J.W. Ochterski, P.Y. Ayala, K. Morokuma, G.A. Voth, P. Salvador, J.J. Dannenberg, V.G. Zakrzewski, S. Dapprich, A.D. Daniels, M.C. Strain, O. Farkas, D.K. Malick, A.D. Rabuck, K. Raghavachari, J.B. Foresman, J.V. Ortiz, Q. Cui, A.G. Baboul, S. Clifford, J. Cioslowski, B.B. Stefanov, G. Liu, A. Liashenko, P. Piskorz, I. Komaromi, R.L. Martin, D.J. Fox, T. Keith, M.A. Al-Laham, C.Y. Peng, A. Nanayakkara, M. Challacombe, P.M.W. Gill, B. Johnson, W. Chen, M.W. Wong, C. Gonzalez, J.A. Pople, Gaussian 03, Revision C.02, Gaussian, Inc., Wallingford, CT, 2004.